EDGE ARTICLE

Multi-electron reduction of sulfur and carbon disulfide using binuclear uranium(III) borohydride complexes†

Polly L. Arnold,*[a] Charlotte J. Stevens,[a] Nicola L. Bell,[a] Rianne M. Lord,[a] Jonathan M. Goldberg,[b] Gary S. Nichol[a] and Jason B. Love*[a]

The first use of a dinuclear U^{III}/U^{III} complex in the activation of small molecules is reported. The octadentate Schiff-base pyrrole, anthracene-hinged 'Pacman' ligand L^A combines two strongly reducing U^{III} centres and three borohydride ligands in $[M(THF)_4][\{U(BH_4)\}_2(\mu\text{-}BH_4)(L^A)(THF)_2]$ 1-M, (M = Li, Na, K). The two borohydride ligands bound to uranium outside the macrocyclic cleft are readily substituted by aryloxide ligands, resulting in a single, weakly-bound, encapsulated *endo* group 1 metal borohydride bridging the two U^{III} centres in $[\{U(OAr)\}_2(\mu\text{-}MBH_4)(L^A)(THF)_2]$ 2-M (OAr = $OC_6H_2{}^tBu_3\text{-}2,4,6$, M = Na, K). X-ray crystallographic analysis shows that, for 2-K, in addition to the *endo*-BH_4 ligand the potassium counter-cation is also incorporated into the cleft through η^5-interactions with the pyrrolides instead of extraneous donor solvent. As such, 2-K has a significantly higher solubility in non-polar solvents and a wider U–U separation compared to the 'ate' complex 1. The cooperative reducing capability of the two U^{III} centres now enforced by the large and relatively flexible macrocycle is compared for the two complexes, recognising that the borohydrides can provide additional reducing capability, and that the aryloxide-capped 2-K is constrained to reactions within the cleft. The reaction between 1-Na and S_8 affords an insoluble, presumably polymeric paramagnetic complex with bridging uranium sulfides, while that with CS_2 results in oxidation of each U^{III} to the notably high U^V oxidation state, forming the unusual trithiocarbonate $(CS_3)^{2-}$ as a ligand in $[\{U(CS_3)\}_2(\mu\text{-}\kappa^2\text{:}\kappa^2\text{-}CS_3)(L^A)]$ (4). The reaction between 2-K and S_8 results in quantitative substitution of the *endo*-KBH_4 by a bridging persulfido $(S_2)^{2-}$ group and oxidation of each U^{III} to U^{IV}, yielding $[\{U(OAr)\}_2(\mu\text{-}\kappa^2\text{:}\kappa^2\text{-}S_2)(L^A)]$ (5). The reaction of 2-K with CS_2 affords a thermally unstable adduct which is tentatively assigned as containing a carbon disulfido $(CS_2)^{2-}$ ligand bridging the two U centres (6a), but only the mono-bridged sulfido $(S)^{2-}$ complex $[\{U(OAr)\}_2(\mu\text{-}S)(L^A)]$ (6) is isolated. The persulfido complex (5) can also be synthesised from the mono-bridged sulfido complex (6) by the addition of another equivalent of sulfur.

Introduction

The U^{III} oxidation state is strongly reducing and its molecular complexes are well known for their ability to activate small molecules[1–3] such as arenes,[4,5] N_2,[6–10] CO,[11–19] and CO_2.[20–26] The coordination of actinides with chalcogenide ligands has begun to attract increasing interest.[27–33] Understanding and controlling the activation and functionalisation of chalcogen elements and their compounds is important in the petroleum industry

and in functional polymer technologies, and is increasingly of interest for new methods in organic and biomimetic syntheses,[34] both with d-block[35–43] and rare earth metal[44,45] complexes. The kinetically facile nature of the soft atom transfer reactions with the harder metal cations suggests opportunities in catalytic chalcogen atom-transfer processes, yet the binding mode and stoichiometry of the incorporated chalcogen atoms/fragments is as yet unpredictable and so far appears to be primarily dependent on subtle differences in steric accessibility of the reducing metal centre(s). Furthermore, complexes that exhibit different binding modes with polarisable atoms such as these can provide new insight into the role of f- and other valence orbitals in actinide-ligand bonding which is fundamentally important to improving the safe handling of nuclear waste materials.[46–49]

Almost all instances of the activation of sulfur or sulfur-containing small molecules by an actinide involve the assembly of two mononuclear U^{III} centres around one or more

[a]EaStCHEM School of Chemistry, University of Edinburgh, The King's Buildings, Edinburgh EH9 3JF, UK. E-mail: Polly.Arnold@ed.ac.uk; Jason.Love@ed.ac.uk; Fax: +44 (0)131 6506453; Tel: +44 (0)131 6505429

[b]Department of Chemistry, University of Washington, Box 351700, Seattle, WA 98195-1700, USA

† Electronic supplementary information (ESI) available: Full synthetic and structural characterisation data. CCDC 1480072–1480076. For ESI and crystallographic data in CIF or other electronic format see DOI: 10.1039/c7sc00382j

atoms of elemental sulfur, or an S atom from CS_2, providing two reducing electrons to form $[U^{IV}]_2$ products, occasionally with further incorporation of CS_2. Products are often formed as a mixture of the persulfido $(E_2)^{2-}$-bridged $[U^{IV}]_2$ complexes such as $(\mu-\eta^2:\eta^2-S_2)[UX_3]_2$ (where $[UX_3] = [U(C_5H_4Me)_3]$,[47] $[U(N''_3)_3]$ ($N'' = N(SiMe_3)_2$),[27] $[U\{(SiMe_2NPh)_3tacn\}]$,[50] and $[U\{(^{Ad}ArO)_3$-tacn\}]$,[51]), and sulfido $(E)^{2-}$-bridged $[U^{IV}]_2$ complexes such as $(\mu-S)[U(N''_3)_3]_2$,[27] and $(\mu-S)[U((SiMe_2NPh)_3tacn)]_2$.[50] The first terminal uranium persulfido complex was $U[(SiMe_2NPh)_3$-tacn](η^2-S_2).[50] Incorporation of up to four S atoms has also been observed, e.g. in $[K(18-crown-6)][(\eta^n-S_n)U(N''_3)_3]$ ($n = 1-3$),[52] and $(\mu-S_2)_2[U\{(^{Ad}ArO)_3tacn\}]_2$.[51] One monosulfido complex adds CS_2 to form the $[U^{IV}]_2CS_3$ adduct $(\mu-\kappa^2:\kappa^2-CS_3)_2$-$[U\{(^{Ad}ArO)_3tacn\}]_2$, which can also be formed directly from the U^{III} precursor and CS_2. Finally, the 'ate' U^{III} siloxide complex $[K(18-c-6)U\{OSi(O^tBu)_3\}_4]$ has been shown to react with CS_2 to form a variety of potassium-bound reduction products including $[K_2(18-c-6)_2U\{OSi(O^tBu)_3\}_4(\mu^3-\kappa^2:\kappa^2:\kappa^2-CS_3)]$.[53]

We reasoned that the preorganisation of two U^{III} centres could enhance the rate and selectivity of small molecule activation reactions in the now two-body problem. In light of this we reported the first structurally characterised binuclear $[U^{III}]_2$ complex of a single ligand using the small cavity macrocycle trans-calix[2]benzene[2]pyrrole.[54] We further showed that the reaction between $[U(BH_4)_3(THF)_2]$ and the anions of the 'Pacman'-shaped Schiff-base polypyrrolic macrocycles[55–57] afforded another two classes of molecule that combine two U^{III} centres in a single ligand structure.[58] The larger of the two 'Pacman' ligands, hinged by

anthracenyl groups, forms the unusual 'ate' complex, $[Na(THF)_4]$ $[\{U^{III}(BH_4)\}_2(\mu-BH_4)(L^A)(THF)_2]$ **1-Na**, Scheme 1.[58]

Herein, we report reactivity studies of **1** and a new derivative in which the exo-coordination sites of both U^{III} centres are protected by 'capping' aryloxide groups. We demonstrate the differences in reactivity between these compounds and their unique selectivity for the formation of $(\mu-S)$, $(\mu-S_2)$ or $(\mu-CS_3)$ in their reactions with S_8 and CS_2.

Results and discussion

The reaction of H_4L^A with $KN(SiMe_3)_2$, followed by $U(BH_4)_3(THF)_2$ affords $[K(THF)_4][\{U^{III}(BH_4)\}_2(\mu-BH_4)(L^A)(THF)_2]$ **1-K** in good yield; **1-K** is the potassium analogue of our recently reported sodium complex **1-Na**.[56,59] Reactions of **1-K** to target exo-X ligand substitution with amide, alkoxide, aryloxide, cyclopentadienyl, alkyl and allyl anions were investigated (see ESI†).

The most successful reactions, as evidenced by ^1H NMR spectroscopy are those between **1-K** and two equivalents of the aryloxide MOAr where M = K, Na and Ar = $C_6H_2(^tBu)_3$-2,4,6 (Scheme 1). The ^1H NMR spectra of both reaction mixtures are very similar and each display a new set of very broad, para-magnetically shifted resonances of low intensity, which nevertheless are consistent with a single, symmetric macrocyclic ligand environment. A large quantity of dark green crystals formed over 4 h in the **1-Na**/KOAr reaction mixture. Analysis of these by X-ray diffraction revealed their composition to be $[\{U(OAr)\}_2(endo-\mu-KBH_4)(L^A)(THF)_2]$ (**2-K**) in which the two exo BH_4^- ligands have been exchanged for aryloxides and the Na^+ cation of **1-Na** has been exchanged for a K^+ cation which notably now binds within the macrocyclic cleft (Fig. 1). Single crystals also formed in the **1-Na**/NaOAr reaction mixture, but only after standing for two weeks. These were characterised as the analogous Na^+-containing product $[\{U(OAr)\}_2(endo-\mu-NaBH_4)(L^A)(THF)_2]$ (**2-Na**) in which again the Na^+ cation is also located within the macrocyclic cleft (Fig. 1). The in situ NMR scale reaction between **1-K** and NaOAr yielded resonances consistent with the formation of only **2-K**. Interestingly, no reaction occurs between **1-K** and two equivalents of LiOAr. On a preparative scale, the reaction of **1-Na** with KOAr in THF allows crystalline **2-K** to be isolated in 59% yield. Crystalline **2-K** is insoluble in THF and pyridine but sparingly soluble in toluene and hot benzene. The ^1H NMR spectrum of **2-K** in C_6D_6 is sharper than that of the crude product formed from an in situ synthesis in d_8-THF and contains paramagnetically shifted resonances corresponding to a symmetric macrocycle and two equivalent aryloxide ligands. One resonance that integrates to 18H is seen at 4.1 ppm for the two para-^tBu groups and one of integral 36H at -0.1 ppm for the four ortho-^tBu groups of the two aryloxides. The resonance corresponding to the four equivalent meta protons of the aryloxides cannot be distinguished from the macrocycle resonances of equal integral. A single broad resonance appears in the ^{11}B NMR spectrum at 188 ppm, attributed to the endo-KBH_4, in comparison to the two resonances seen at 212 ppm (1B, endo-BH_4) and 207 (2B, exo-BH_4) for **1-K**. The solution state IR for complex **2-K** in THF shows a single stretch at 2280 cm^{-1} corresponding to a symmetric $U(\mu^2-\eta^2-, \mu^2-\eta^2-H_2BH_2)U$ ionic
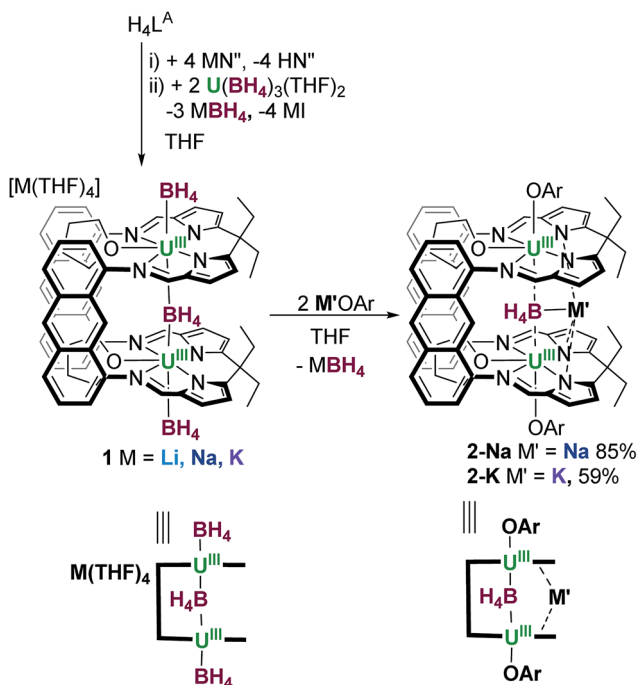
Scheme 1 The reaction of H_4L^A with $M(SiMe_3)_2$ (M = Li, Na, K) and $U(BH_4)_3(THF)_2$ to yield $[Na(THF)_4][\{U(BH_4)\}_2(\mu-BH_4)(L^A)(THF)_2]$ (**1-Na**, previously reported) and the group 1 analogues **1-Li** and **1-K**; further reaction with MOAr yields $[M\{U(OAr)(THF)\}_2(endo-\mu-BH_4)(L^A)]$ (OAr = $OC_6H_2{}^tBu_3$-2,4,6, M = K, **2-K**; M = Na, **2-Na**).
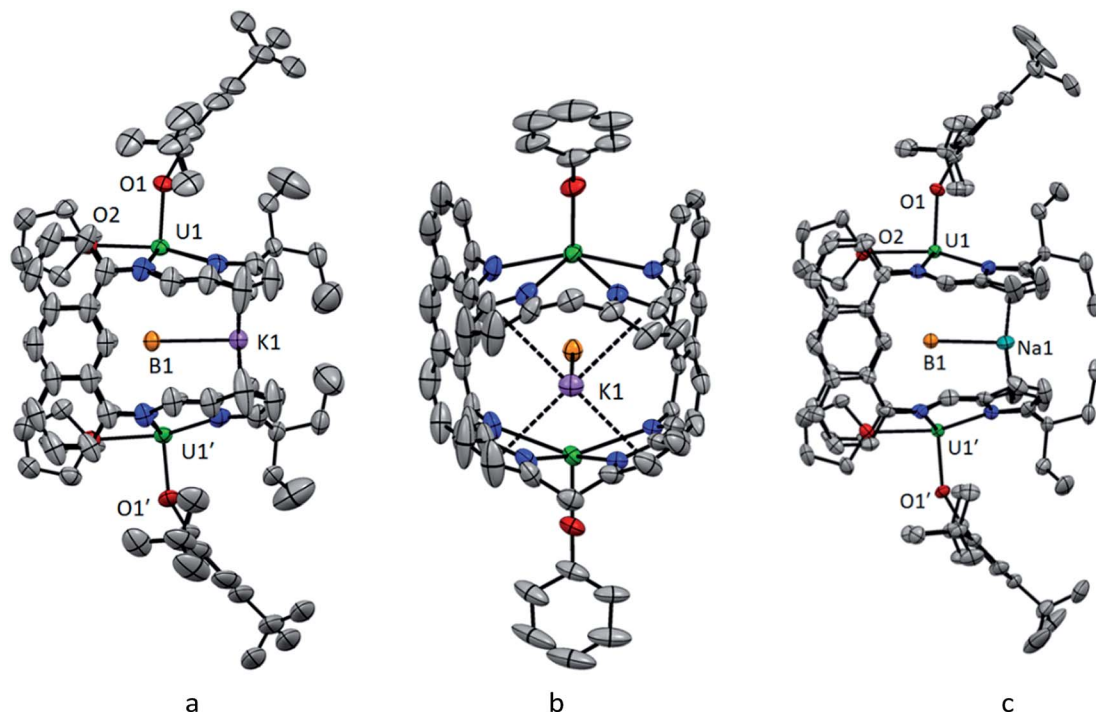
Fig. 1 Solid-state structure of **2-K** showing side view (a) and front view (b), and solid-state structure of **2-Na**, side view (c). For clarity, the major orientation of the disordered ^{t}Bu groups in **2-K** is shown in (a) and the *meso* ethyl groups, aryloxide substituents, THF molecules, and *tert*-butyl groups are omitted from (b); all H atoms and lattice solvent are also omitted (displacement ellipsoids are drawn at 50% probability). Full details for **2-Na** are in the ESI.†

Table 1 Comparison of selected distances (Å) and angles (°) in the structures of **2-K** and **2-Na**

	2-K	**2-Na**
U1⋯U1′	6.5881(3)	6.5265(7)
Mean U–N$_{im}$	2.65	2.65
Mean U–N$_{pyr}$	2.50	2.51
U1–N$_4$ plane	0.70	0.69
U1–O1	2.231(5)	2.245(6)
U1⋯B1	3.312(1)	3.269(1)
U1–O2	2.554(5)	2.592(6)
B1–M1	3.036(11)	2.747(2)
M1-[pyr]centroid	3.154(2), 3.153(2)	2.85(4), 3.04(2), 3.08(4), 3.61(2)
U1–B1–U1′	168.2(4)	173.0(6)
O1–U1–B1	178.3(2)	177.6(1)
U1–O1–C$_{ipso}$	154.0(5)	153.3(6)

binding mode in solution, identical to that observed in the solid state for **1-Na**.

The geometry of each U^{III} centre in **2-K** (Fig. 1) is best described as a distorted pentagonal bipyramid. The coordination environment of the U^{III} centre shows five equatorial donor atoms, comprising the four nitrogen atoms of the macrocycle and one oxygen atom of THF solvent, which sits between the macrocyclic hinges, and the borohydride. The aryloxide ligand occupies the *exo* axial coordination site and the BH$_4$ ligand (hydrogens not located) sits within the macrocyclic cleft bridging the two U^{III} centres with long U–B distances of about 3.3 Å (Table 1).

The phenyl rings of the aryloxide ligands are perpendicular to the anthracenyl hinges of the macrocycle and the angle at the O atom (U1–O1–C$_{ipso}$ = 154.0(5)° (**2-K**), 153.3(6)° (**2-Na**)) orients the *ortho-*^{t}Bu groups away from the THF donor. The U^{III} cations are considerably displaced out of the macrocycle N4 donor planes, away from the intermetallic cleft, by 0.70 Å in **2-K** and 0.69 Å in **2-Na**, and the sum of the four N–U–N angles in the two structures is 337.9(8)° and 338.1(8)° respectively. The separation of the bulky aryloxide ligand from the N4 plane of the macrocycle is imposed by steric demand. Therefore, the displacement of the U^{III} centres out of the N4 plane is a compromise between optimised U–OAr and U–N bond lengths. The resulting mean U–N(imine) distances of 2.65 Å in both complexes and the mean U–N(pyrrolide) distances of 2.50 Å (**2-K**) and 2.51 Å (**2-Na**) are lengthened compared to those observed in **1-Na** (2.62 Å and 2.49 Å). The U1–O1 bond lengths in **2-K** and **2-Na** are 2.231(5) Å and 2.245(6) Å respectively (Table 1). These are longer than the U^{III}-OAr distances in $[U(OC_6H_3{}^iPr_2-2,6)_3]$[54] and $[U(OC_6H_3{}^tBu_2-2,6)_3]$[59] which range from 2.149(4) to 2.214(7) Å but similar to the mean U-OAr distance of 2.22 Å observed in the constrained aryloxide TACN complexes $U[(^RArO)_3(TACN)]$.[60,61]

The main difference between the structures of **2-K** and **2-Na** is the binding of the K$^+$ and Na$^+$ cations within the cleft. The larger K$^+$ ion is sandwiched symmetrically between all four pyrrolide rings (Fig. 1a) with K1-[pyr]centroid separations of 3.154(2) Å and 3.153(2) Å. By contrast, the smaller Na$^+$ ion is disordered over two sites about the crystallographic C_2 axis, presumably because it cannot effectively bridge all four

pyrrolides. This results in three shorter Na1-[pyr]centroid distances of 2.85(4), 3.04(2) and 3.08(4) Å and one long, non-bonding separation of 3.61(2) Å (Fig. 1c). The larger and more polarisable K^+ is clearly a better match for the Pacman macro-cyclic cleft than Na^+. Based on the M1···B1 separations, the U ions form a standard bonding interaction with the BH_4 anion.[62,63] Reported terminal $K···BH_4$ separations range from 2.947(3)[64] to 3.091(4)[65] Å with a mean value of 3.00 Å, while terminal $Na···BH_4$ separations range from 2.600(6)[66] to 2.841(2)[67] Å with a mean value of 2.68 Å. The K1–B1 (3.036(11) Å) and Na1–B1 (2.747(2) Å) separations in **2-K** and **2-Na** lie within these ranges, close to the mean values. The elongated K1–B1 distance means that the BH_4^- ligand sits further back into the molecular cleft in **2-K** and the U1–B1–U1′ angle in **2-K** (168.2(4)°) is more acute than that in **2-Na** (173.0(6)°).

The effect of the out-of-cleft distortion of the U^{III} centres is a marked lengthening of both the U···U and the U···(endo-BH_4) separations. The U1···U1′ separation is 6.5881(3) Å in **2-K** and 6.5265(7) Å in **2-Na** compared to 5.9243(3) Å in **1-Na**. U1–B1 is 3.312(1) Å in **2-K** and 3.269(1) in **2-Na** compared to 2.977(7) Å and 2.949(7) Å in **1-Na**. The U–B distances in **2** are the longest observed for any uranium borohydride complex, with the next longest being complex **1-Na** followed by 2.927(7) Å in [U(BH$_4$)L′] (L′ = trans-calix[2]benzene[2]pyrrolide).[59] This raises the question of whether there is a bond between the U^{III} ions and the endo BH_4^- group in **2-K** and **2-Na** or whether the BH_4^- group is held within the cleft by association with its M^+ counter-ion. The observed ^{11}B NMR shift of the endo BH_4^- group in **2-K** (188 ppm) is significantly para-magnetically shifted from that of free KBH_4 (−40 ppm) indicating that there is some electronic overlap between the U^{III} centres and the BH_4^- group in solution. Therefore, it is likely that in-cleft cation binding in **2-K** and **2-Na** contributes to the stabilisation of a very weak and long U(BH$_4$)–U interaction.
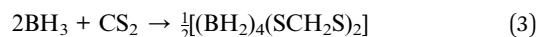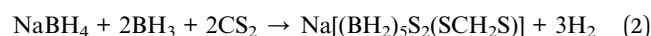
Reactions of 1 and 2

Reactions to compare the small molecule activation chemistry of **1-Na** and **2-K** were carried out, noting both the high number of potential reducing equivalents in **1** and the weak binding of the central, and unsolvated MBH_4 in **2**.

Complex **1-Na** was dissolved in THF and 0.75 equivalents of S_8 was added, immediately forming a red solution of a product we assign as [U$_2$S$_3$(L^A)]$_n$ **3** from elemental analysis, and analysis of the boron–sulfur containing by-products of the reaction, Scheme 2. The ^1H NMR spectrum of a freshly made solution shows paramagnetically shifted resonances between +34 and −23 ppm that correspond to a symmetrical macrocycle environment; some H_2 is also seen in solution. The ^{11}B NMR spectrum contains two triplets in a 4 : 1 ratio at −6.2 and −16.5 ppm, the latter of which can be assigned to Na$_2$[(BH$_2$)$_6$S$_4$], the caesium analogue of which has previously been made from the reaction between $CsBH_4$, BH_3 and H_2S (eqn (1)).[68] The initially-soluble reaction product precipitates from the reaction mixture over a 12 h period and remains insoluble in common polar aprotic solvents. This observation and the rarity with which S binds as a terminal multiply bonded ligand led us to assign a polymeric structure for **3** as drawn in Scheme 2.

$$CsBH_4 + 2THF{:}BH_3 + 2H_2S \rightarrow \tfrac{1}{2}Cs_2[(BH_2)_6S_4] + 4H_2 \quad (1)$$
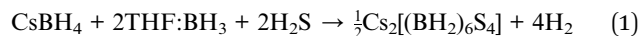
A THF solution of **1-Na** was treated with an excess (>9 equivalents) of CS_2, upon which the reaction mixture immediately turned bright orange, and quantitative deposition of the product characterised as [{U(CS$_3$)}$_2$(μ-κ^2:κ^2-CS$_3$)(L^A)] **4** as an orange solid is observed after ca. 15 min. The ^1H NMR spectrum of the reaction mixture before precipitation shows a single symmetrical paramagnetically shifted macrocycle environment with resonances between +25 and −44 ppm. The IR spectrum of solid **4** shows no absorptions in the region 2500–2000 cm^{-1} confirming that no borohydride ligands remain. The ^{11}B NMR spectrum of the supernatant shows two sharp singlets at 0.29 and 0.5 ppm, attributed to boron-sulfide-containing by-products, and shows that the BH_4 ligands have provided additional reducing capability to the U^{III} centres in **1**. Related borohydride reduction reactions from simple group 1 salts are shown in eqn (2)–(5). Both resonances appear at a higher frequency than known reaction products of $NaBH_4$ and BH_3 with CS_2, namely [CH$_2$(BH$_2$)$_5$S$_4$]$^-$ (−13.7/15.8 ppm)[69] and [(BH$_2$)$_4$(SCH$_2$S)$_2$] (−17.0 ppm).[70] The ^{11}B NMR resonance at 0.5 ppm is attributed to the known anion [B(SCH$_2$S)$_4$]$^{5-}$ (eqn (4)) which is formed from the sub-stoichiometric reaction of $NaBH_4$ with CS_2. The corresponding CH_2 group is observed as a quartet at 3.97 ppm in the ^1H NMR spectrum.[71] The second species in the ^{11}B NMR appears closer to the polymeric species, formulated as {[B(SCH$_2$S)$_2$]$^-$}$_n$ (0.0 ppm, eqn (5)) suggesting a similar formulation for the resonance at 0.29 ppm possibly with an intermediate charge (e.g. [B(SCH$_2$S)$_3$]$^{3-}$).[71]

$$NaBH_4 + 2BH_3 + 2CS_2 \rightarrow Na[(BH_2)_5S_2(SCH_2S)] + 3H_2 \quad (2)$$

$$2BH_3 + CS_2 \rightarrow \tfrac{1}{2}[(BH_2)_4(SCH_2S)_2] \quad (3)$$

$$5NaBH_4 + 4CS_2 \rightarrow Na_5[B(SCH_2S)_4] + 2B_2H_6 \quad (4)$$

$$NaBH_4 + 2CS_2 \rightarrow \{Na[B(SCH_2S)_2]\}_n \quad (5)$$

Small orange crystals of [{U(CS$_3$)}$_2$(μ-κ^1:κ^1:κ^2-CS$_3$)(L^A)] **(4)** were obtained from the concentrated THF solution. X-ray crystallographic analysis of **4** shows the incorporation of the rare trithiocarbonate (CS$_3$)$^{2-}$ motif in the endo and both of the exo uranium coordination sites from which charge balancing arguments assign the notably high formal oxidation state of U^V/U^V (Fig. 2). While the crystallographic data are poor and prevent a full discussion of structural parameters, the U···U separation is 5.85 Å (from an average of the three structures in the unit cell). This is the first case in which two uranium centres have been shown to provide a total of four reducing electrons (rather than just one each) in the rare formation of the (CS$_3$)$^{2-}$ ligand, and the first time that more than one thiocarbonate ligand has been formed through reductive activation by a single molecule.

The reactivity of the more soluble complex **2-K** provides an interesting comparison with that of **1-M**. Reactions of **2-K** were carried out with both S_8 and CS_2 in the anticipation of displacing the single, weakly bound endo-KBH_4 molecule.
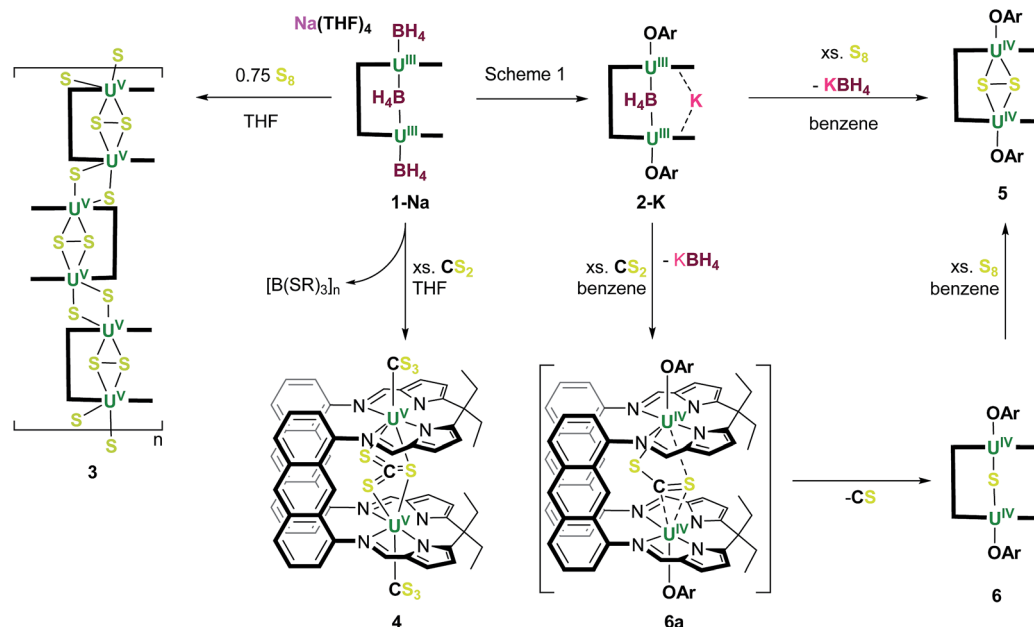
Scheme 2 Contrasting reactions of $[Na(THF)_4][\{U(BH_4)\}_2(\mu\text{-}BH_4)(L^A)(THF)_2]$ (**1-Na**) and $[\{U(OAr)(THF)_2\}_2(endo\text{-}\mu\text{-}KBH_4)(L^A)]$ (**2-K**) and the synthesis of complexes **3–6** (OAr = $OC_6H_2{}^tBu_3\text{-}2,4,6$).
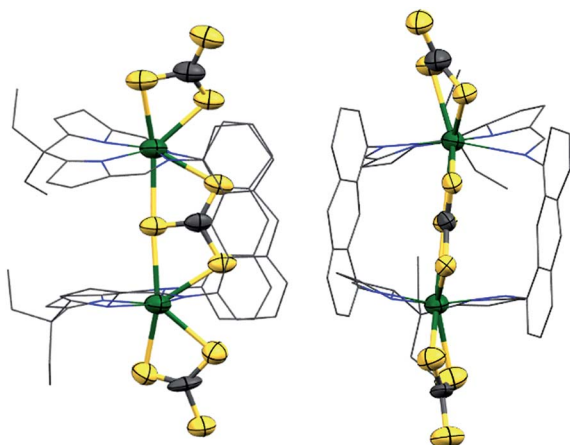

Fig. 2 Solid-state structure of **4** showing side view (left) and front view (right). Due to poor quality data, the structure could not be refined adequately so only connectivity is described. All atoms were refined isotropically except the uranium atoms and those in the $CS_3{}^{2-}$ units. For the anisotropic atoms, displacement ellipsoids are drawn at 50% probability. For clarity, H-atoms are omitted and isotropic atoms are shown as wireframe. Colour code: green = uranium, yellow = sulfur, blue = nitrogen, grey = carbon.

Addition of an excess of S_8 to a slurry of **2-K** in toluene resulted in the immediate formation of a pale orange solution and a pale yellow precipitate of KBH_4. Addition of hexanes to the filtrate results in the deposition of orange crystals of the thermally stable product $[\{U(OAr)\}_2(\mu\text{-}\kappa^2{:}\kappa^2\text{-}S_2)(L^A)]$ (**5**) in 41% yield (Scheme 2). In the solid-state structure (Fig. 3) the intermetallic cleft is occupied by a bridging persulfido ion, $(S_2)^{2-}$, suggesting that both uranium centres have been oxidised to U^{IV}. This is reinforced by the reduction of the U–L bond lengths (*cf.*

2-K), in keeping with the values for known U^{IV} complexes (see below). The ^1H NMR spectrum of a solution of **5** displays paramagnetically shifted resonances corresponding to a single C_2-symmetric macrocycle environment and two equivalent aryloxide ligands, as was observed in the ^1H NMR spectrum of **2-K**. However, in contrast to **2-K**, the aryloxide rings appear to be rotating freely in solution as only three resonances in a 36 : 18 : 4 ratio are seen. No resonances are seen in the ^{11}B
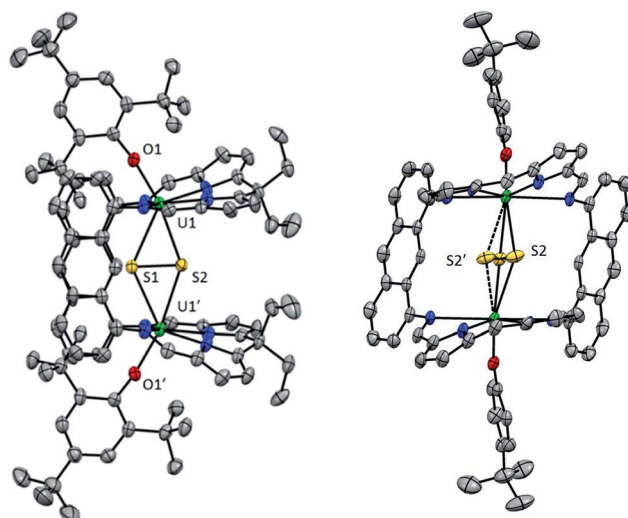

Fig. 3 Solid-state structure of **5** showing side-on view (left) and front view (right). The alternative, symmetry generated S2 position, S2′ (dashed bonds), is only shown in the right hand structure. For clarity, all H atoms and lattice solvent are omitted, along with the macrocycle *meso* ethyl groups and aryloxide *ortho* ^tBu groups from the right-hand view (displacement ellipsoids are drawn at 50% probability).

NMR spectrum confirming the loss of KBH_4 from the cleft and its subsequent precipitation.

Addition of an excess of CS_2 to a suspension of **2-K** in d_8-toluene results in a slow colour change from dark green to orange-brown over the course of 10 min and formation of an orange precipitate (Scheme 2). The solution species were characterised on the basis of NMR spectroscopy as $[\{U(OAr)\}_2(\mu\text{-}CS_2)(L^A)]$ (**6a**) and $[\{U(OAr)\}_2(\mu\text{-}S)(L^A)]$ (**6**). The resonances of the major species **6a** indicate the presence of a single asymmetric macrocyclic compound in which the two compartments of the macrocycle are inequivalent. The two aryloxide ligands are also inequivalent; nine resonances are observed, five of intensity 9H corresponding to five of the six ^{t}Bu groups (the resonance of the sixth group is assumed to be concealed by the solvent resonances) and four of intensity 1H corresponding to each *meta* proton. It is proposed from this that both aryloxide ligands are rigidly bound with the aryl rings coplanar with the anthracenyl groups of the macrocycle hinge. As no resonances are seen in the ^{11}B NMR spectrum, it is probable that displacement of KBH_4 by CS_2 has occurred, and that a bent $(CS_2)^{2-}$ unit binds asymmetrically between the two U^{IV} centres, rendering the macrocyclic compartments and *exo* aryloxides inequivalent. Complex **6a** is not stable in solution, and converts quantitatively to a new, C_2-symmetric complex either on standing at room temperature for five days or heating in benzene for 2.5 h; the resulting complex was characterised as the orange sulfido-bridged compound $[\{U(OAr)\}_2(\mu\text{-}S)(L^A)]$ (**6**) (see below). No further reactivity of **6** with CS_2 was observed, but boiling a benzene solution of **6** and excess S_8 resulted in the formation of an orange solution which showed resonances in the ^{1}H NMR spectrum corresponding to complex **5**, Scheme 2.

By comparing the reactions of **1** and **2-K** with excess CS_2, it is seen that the *exo*-aryloxide groups direct the uranium centres to activate only one molecule of CS_2 within the cleft, forming **6a** initially and eventually the sulfido-bridged **6**. However, without the aryloxide capping ligands, **1** is able to activate CS_2 in both the *exo* and *endo* positions, with poor overall control, resulting in the formation of poorly soluble products.[67]

X-ray crystal structures of the *endo*-chalcogenido complexes 5 and 6

Orange single crystals of **5** suitable for X-ray structural analysis were obtained from a C_6D_6/hexane solution. In the solid-state, the U^{IV} cations in **5** are seven coordinate, binding to the four N donors of the macrocycle, the *exo*-aryloxide ligand and both S atoms of the *endo*-bridging persulfido ion (Fig. 4). The solid-state structure of **5** confirms that, in contrast to **2**, the aryloxide rings are indeed approximately coplanar with the anthracene hinges of the macrocycle with one *ortho*-^{t}Bu group on each ring sitting between the hinges. Also, the two THF molecules which were bound to the U centres in the equatorial sites in **2-K** have dissociated during formation of **5**. The U1–O1 bond length in **5** is 2.091(3) Å, which is reduced from 2.231(5) Å in **2-K** and supports the oxidation of the U^{III} centres to U^{IV}. The angle at the O atom of the aryloxides (U1–O1–C_{ipso} = 169.0(3)°) is less acute than that observed in **2-K** (154.0(5)°). The mean U1–
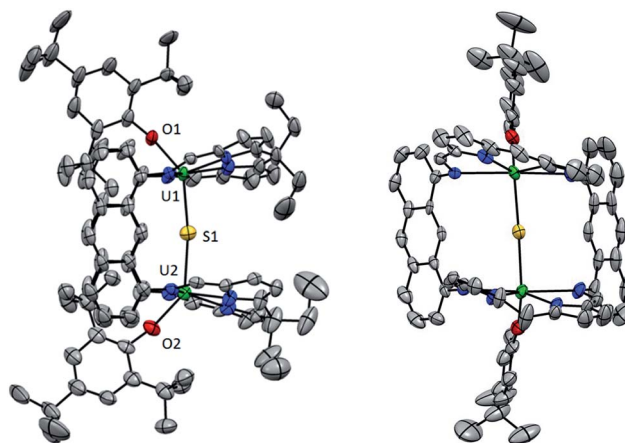

Fig. 4 Solid-state structure of **6** showing side view (left) and front view (right). For clarity, all H atoms and lattice solvent are omitted along with the *meso* ethyl groups and aryloxide *ortho* ^{t}Bu groups from the right-hand drawing (displacement ellipsoids are drawn at 50% probability).

Table 2 Selected structural parameters of complexes **5** and **6**

	5	6
U1⋯U1′	5.1571(5)	5.1899(5)
Mean U–N_{im}	2.63	2.59
Mean U–N_{pyr}	2.41	2.42
U–N_4 plane	−0.07	−0.10/−0.03
U–O	2.091(3)	2.081(6)/2.099(6)
U1–S1	2.8229(8)	2.608(2)/2.594(2)
U1–S2	2.707(3)	
S1–S2	2.118(3)	
O1–U1–S1	125.7(1)	140.1(2)/143.2(2)
O1–U1–S2	166.6(1)	
U1–S1–U1′	131.98(7)	
U1–S2–U1′	135.0(1)	172.0(1)
S1–S2–U1	70.40(8)	
S2–S1–U1	64.62(8)	
U1–(S_2)cent–U1′	165.4	
U1–O1–C_{ipso}	169.0(3)	170.4(5)/167.8(6)

N(pyrrolide) distance has contracted from 2.50 Å in **2-K** to 2.41 Å in **5**, though the difference in the mean U1–N(imine) distances is less marked (Table 2).

The $(S_2)^{2-}$ unit in **5** is symmetry defined to be equidistant from the two U^{IV} centres but the U1–S1 bond length of 2.8229(8) Å is longer than the U1–S2 length of 2.707(3). S2 is disordered over two sites related by rotation about the C_2 axis and the occupancy of each site was fixed at 0.5. U1, U1′, S1 and S2 are not coplanar but instead the $\{U_2S_2\}$ unit forms a bent diamond with a dihedral angle of 165.4°. Bridging persulfido uranium complexes are rare, with the only two examples having been reported very recently, and both featuring a persulfido ion bridging symmetrically between two U^{IV} centres in $[\{U(N\{SiMe_3\}_2)_3\}_2(\mu\text{-}\kappa^2\text{:}\kappa^2\text{-}S_2)]$[27] and $[\{U((SiMe_2NPh)_3TACN)\}_2(\mu\text{-}\kappa^2\text{:}\kappa^2\text{-}S_2)]$.[50]

Orange block-shaped crystals of **6** suitable for X-ray crystallography were obtained by addition of hexanes to a toluene solution (Fig. 4). The coordination environment about the two

U^{IV} ions in **6** is distorted octahedral and the four N donors of the macrocycle occupy the equatorial plane with the *exo* aryloxide and *endo* bridging sulfido ligands axial. There is, however, a large deviation from idealised octahedral geometry; the angles between the *trans* axial ligands O1–U1–S1 and O2–U2–S2 are 143.2(2)° and 140.1(2)°, respectively. As with **5**, the aryloxides are tilted back toward the hinges of the macrocycle to avoid unfavourable steric interactions between their *ortho*-^{t}Bu groups and the *exo meso* ethyl groups of the macrocycle. At 2.594(2) Å and 2.608(2) Å, the U–S bond lengths in **6** are reduced by *ca.* 0.16 Å compared to the mean U–S distance observed in the persulfido complex **5** (Table 2).

The geometry of the {U-(μ-S)-U} core in **6** is approaching linear (U1–S1–U2 is 172.0(1)°) and the U1$\cdots$U2 separation is 5.1899(5) Å. Other mono-sulfido bridged complexes prepared to date include [{U(N{SiMe$_3$}$_2$)$_3$}$_2$(μ-S)][27] [{U(OAr)$_3$}$_2$(μ-S)] (Ar = 2,6-C$_6$H$_3$(^{t}Bu)$_2$)[65] and [{U((AdArO)$_3$N)(DME)}$_2$(μ-S)].[66] In these compounds the U–S bond lengths range from 2.588(1) Å to 2.736(2) Å, the U$\cdots$U separations vary from 5.176(3) Å to 5.4407(6) Å and the U–S–U angles range from 165.2(2)° to 180°. The structural parameters of the {U-(μ-S)-U} unit in **6** lie within these limits and so the rigid environment of the Pacman macrocycle does not appear to cause an excessive distortion.

We attribute the formation of complex **6** to the slow reductive cleavage of the bound CS$_2$ molecule in **6a** to form S^{2-} and release CS. This is an unusual transformation since CS is not expected to be stable, and so not prone to eliminate, in contrast to reactions of CO$_2$ with reducing metal complexes that often eliminate CO and form an oxo bridge.[72,73] Despite this, CS formed from reductive disproportionation of CS$_2$ has been trapped previously.[43,74] To probe whether this transformation is accelerated by heating, a solution of **6a** in C$_6$D$_6$ was boiled for 2.5 hours forming an orange solution and a brown precipitate. The subsequent ^{1}H NMR spectrum displayed one major set of paramagnetically shifted resonances assignable to a single, symmetric Pacman product consistent with the transformation of **6a** into **6**. The ^{1}H NMR spectrum of **6** exhibits just five aryloxide resonances in the ratio 18 : 18 : 18 : 2 : 2, as was seen for the similarly symmetric persulfido complex **5**.

Conclusions

The reactions of [Na(THF)$_4$][{U(BH$_4$)}$_2$(μ-BH$_4$)(L^A)(THF)$_2$] (**1-Na**) with two equivalents of MOAr (where M = K or Na and OAr = OC$_6$H$_2$^{t}Bu$_3$-2,4,6), result in the exclusive substitution of the *exo*-BH$_4$ for an aryloxide, yielding [{U(OAr)}$_2$(*endo*-BH$_4$M)(L^A)(THF)$_2$] (K = **2-K** and Na = **2-Na**). An unusual binding mode for MBH$_4$ is seen in which the M$^+$ counter-ion sits adjacent to the BH$_4$ ligand in a cavity formed by the π-systems of four pyrrolide rings of the macrocycle. The U$\cdots$U separation is increased by over 0.6 Å, presumably due to this additional *endo*-bound ion pair.

The reaction of [Na(THF)$_4$][{U(BH$_4$)}$_2$(μ-BH$_4$)(L^A)(THF)$_2$] (**1-Na**) with excess S$_8$ formed an insoluble paramagnetic species **3**, with a molecular formula suggesting the formation of a bridging uranium(v) sulfido coordination polymer. In addition, treatment of **1-Na** with CS$_2$ results in the formation of [{U(CS$_3$)}$_2$(μ-η^1:η^1:η^2-CS$_3$)(L^A)] (**4**) in which unusual

trithiocarbonate (CS$_3$)$^{2-}$ motifs are seen in both the *endo* and *exo* positions. To our knowledge, this is the first case in which two uranium(III) centres have been able to provide a total of four reducing electrons rather than just one each in the rare incorporation of the (CS$_3$)$^{2-}$ ligand, and the first time that more than one thiocarbonate has been formed through reductive activation by a single molecule.

The larger cleft size and more loosely-bound *endo*-BH$_4$ in **2** also provides a good site for the activation of S$_8$ and CS$_2$, affording the *endo*-(S$_2$)$^{2-}$ [{U(OAr)}$_2$(μ-η^2:η^2-S$_2$)(L^A)] (**5**) and *endo*-(S)$^{2-}$ [{U(OAr)}$_2$(μ-S)(L^A)] (**6**) complexes, respectively. It is clear that the addition of the aryloxide ligand in **2-K** promotes the activation of the CS$_2$ exclusively between the two U^{III} centres. In contrast, when the aryloxides are not present *i.e.* in **1**, the BH$_4$ groups are easily replaced and activation of CS$_2$ occurs in both the *exo* and *endo* positions. Therefore, to control and localise the activation of CS$_2$, the *exo* aryloxide ligands are essential.

The unusual reactivity of **2-K** is attributed to the unique environment imposed by the Pacman macrocycle. It is concluded that the *endo* persulfido ion may be comfortably incorporated in **5** but further incorporation of sulfur is restricted. Similarly, the sulfido ion bridges the U^{IV} centres effectively in **6** but in-cleft formation of the bulky thiocarbonate ion is disfavoured. Similarly to related U^{IV} systems,[49] sulfido **6** can be converted into persulfido **5** by the addition of elemental sulfur, suggesting the optimum cavity size between the two U^{IV} centres that fits this polarisable anion has been found. These first small molecule activations within the di-uranium(III) Pacman cleft exemplify the flexibility of the anthracenyl-hinged macrocycle, with U$\cdots$U separations ranging from 4.1927(3) Å to 6.5881(3) Å, and that the use of different *endo* ligands and bridging modes could lead to a wider application of these systems towards other less readily reducible molecules.

Acknowledgements

Notes and references

1 H. S. La Pierre and K. Meyer, in *Progress in Inorganic Chemistry*, John Wiley & Sons, Inc., 2014, vol. 58, DOI: 10.1002/9781118792797.ch05, pp. 303–416.

2 B. M. Gardner and S. T. Liddle, *Eur. J. Inorg. Chem.*, 2013, 3753–3770.

3 P. L. Arnold, *Chem. Comm.*, 2011, **47**, 9005–9010.

4 S. M. Mansell, B. F. Perandones and P. L. Arnold, *J. Organomet. Chem.*, 2010, **695**, 2814–2821.

5 P. L. Arnold, A. Prescimone, J. H. Farnaby, S. M. Mansell, S. Parsons and N. Kaltsoyannis, *Angew. Chem., Int. Ed.*, 2015, **54**, 6735–6739.

6 P. Roussel and P. Scott, *J. Am. Chem. Soc.*, 1998, **120**, 1070–1071.

7 F. G. N. Cloke and P. B. Hitchcock, *J. Am. Chem. Soc.*, 2002, **124**, 9352–9353.

8 S. M. Mansell, N. Kaltsoyannis and P. L. Arnold, *J. Am. Chem. Soc.*, 2011, **133**, 9036–9051.

9 A. L. Odom, P. L. Arnold and C. C. Cummins, *J. Am. Chem. Soc.*, 1998, **120**, 5836–5837.

10 I. Korobkov, S. Gambarotta and G. P. A. Yap, *Angew. Chem., Int. Ed.*, 2002, **41**, 3433–3436.

11 C. Elschenbroich, *Organometallics*, Wiley-VCH, 2006.

12 J. Parry, E. Carmona, S. Coles and M. Hursthouse, *J. Am. Chem. Soc.*, 1995, **117**, 2649–2650.

13 W. J. Evans, S. A. Kozimor, G. W. Nyce and J. W. Ziller, *J. Am. Chem. Soc.*, 2003, **125**, 13831–13835.

14 I. Castro-Rodriguez and K. Meyer, *J. Am. Chem. Soc.*, 2005, **127**, 11242–11243.

15 O. T. Summerscales, F. G. N. Cloke, P. B. Hitchcock, J. C. Green and N. Hazari, *Science*, 2006, **311**, 829–831.

16 A. S. P. Frey, F. G. N. Cloke, P. B. Hitchcock, I. J. Day, J. C. Green and G. Aitken, *J. Am. Chem. Soc.*, 2008, **130**, 13816–13817.

17 B. M. Gardner, J. C. Stewart, A. L. Davis, J. McMaster, W. Lewis, A. J. Blake and S. T. Liddle, *Proc. Natl. Acad. Sci.*, 2012, **109**, 9265–9270.

18 O. T. Summerscales, F. G. N. Cloke, P. B. Hitchcock, J. C. Green and N. Hazari, *J. Am. Chem. Soc.*, 2006, **128**, 9602–9603.

19 N. Tsoureas, O. T. Summerscales, F. G. N. Cloke and S. M. Roe, *Organometallics*, 2013, **32**, 1353–1362.

20 J.-C. Berthet, J.-F. L. Maréchal, M. Nierlich, M. Lance, J. Vigner and M. Ephritikhine, *J. Organomet. Chem.*, 1991, **408**, 335–341.

21 I. Castro-Rodriguez, H. Nakai, L. N. Zakharov, A. L. Rheingold and K. Meyer, *Science*, 2004, **305**, 1757–1759.

22 O. T. Summerscales, A. S. P. Frey, F. G. N. Cloke and P. B. Hitchcock, *Chem. Commun.*, 2008, 198–200.

23 O. P. Lam, S. C. Bart, H. Kameo, F. W. Heinemann and K. Meyer, *Chem. Commun.*, 2010, **46**, 3137–3139.

24 A.-C. Schmidt, A. V. Nizovtsev, A. Scheurer, F. W. Heinemann and K. Meyer, *Chem. Commun.*, 2012, **48**, 8634–8636.

25 V. Mougel, C. Camp, J. Pécaut, C. Copéret, L. Maron, C. E. Kefalidis and M. Mazzanti, *Angew. Chem., Int. Ed.*, 2012, **51**, 12280–12284.

26 A. R. Fox, S. C. Bart, K. Meyer and C. C. Cummins, *Nature*, 2008, **455**, 341–349.

27 J. L. Brown, G. Wu and T. W. Hayton, *Organometallics*, 2013, **32**, 1193–1198.

28 O. P. Lam, F. W. Heinemann and K. Meyer, *Chem. Sci.*, 2011, **2**, 1538–1547.

29 J. L. Brown, S. Fortier, R. A. Lewis, G. Wu and T. W. Hayton, *J. Am. Chem. Soc.*, 2012, **134**, 15468–15475.

30 W. Ren, G. Zi, D.-C. Fang and M. D. Walter, *J. Am. Chem. Soc.*, 2011, **133**, 13183–13196.

31 L. P. Spencer, P. Yang, B. L. Scott, E. R. Batista and J. M. Boncella, *Inorg. Chem.*, 2009, **48**, 11615–11623.

32 O. P. Lam, S. M. Franke, F. W. Heinemann and K. Meyer, *J. Am. Chem. Soc.*, 2012, **134**, 16877–16881.

33 J. L. Brown, S. Fortier, G. Wu, N. Kaltsoyannis and T. W. Hayton, *J. Am. Chem. Soc.*, 2013, **135**, 5352–5355.

34 L. Wang, W. He and Z. Yu, *Chem. Soc. Rev.*, 2013, **42**, 599–621.

35 M. Draganjac and T. B. Rauchfuss, *Angew. Chem., Int. Ed. Engl.*, 1985, **24**, 742–757.

36 F. A. Cotton and G. Schmid, *Inorg. Chem.*, 1997, **36**, 2267–2278.

37 A. R. Johnson, W. M. Davis, C. C. Cummins, S. Serron, S. P. Nolan, D. G. Musaev and K. Morokuma, *J. Am. Chem. Soc.*, 1998, **120**, 2071–2085.

38 J. S. Figueroa and C. C. Cummins, *J. Am. Chem. Soc.*, 2003, **125**, 4020–4021.

39 A. Kayal, J. Kuncheria and S. C. Lee, *Chem. Commun.*, 2001, 2482–2483.

40 M. C. Kuchta and G. Parkin, *J. Chem. Soc. Chem. Commun.*, 1994, 1351.

41 Q. Zhang, G. Armatas and M. G. Kanatzidis, *Inorg. Chem.*, 2009, **48**, 8665–8667.

42 W. A. Howard, T. M. Trnka and G. Parkin, *Organometallics*, 1995, **14**, 4037–4039.

43 B. Li, X. Tan, S. Xu, H. Song and B. Wang, *J. Organomet. Chem.*, 2008, **693**, 667–674.

44 D. J. Berg, C. J. Burns, R. A. Andersen and A. Zalkin, *Organometallics*, 1989, **8**, 1865–1870.

45 A. Kornienko, J. H. Melman, G. Hall, T. J. Emge and J. G. Brennan, *Inorg. Chem.*, 2002, **41**, 121–126.

46 D. E. Smiles, G. Wu, P. Hrobárik and T. W. Hayton, *J. Am. Chem. Soc.*, 2016, **138**, 814–825.

47 M. Roger, L. Belkhiri, P. Thuéry, T. Arliguie, M. Fourmigué, A. Boucekkine and M. Ephritikhine, *Organometallics*, 2005, **24**, 4940–4952.

48 M. J. Manos and M. G. Kanatzidis, *J. Am. Chem. Soc.*, 2002, **134**, 16441–16446.

49 Q. Wu, B. V. Yakshinskiy, T. Gouder and T. E. Madey, *Catal. Today*, 2003, **85**, 291–301.

50 C. Camp, M. A. Antunes, G. García, I. Ciofini, I. C. Santos, J. Pécaut, M. Almeida, J. Marçalo and M. Mazzanti, *Chem. Sci.*, 2014, **5**, 841–846.

51 S. M. Franke, F. W. Heinemann and K. Meyer, *Chem. Sci.*, 2014, **5**, 942–950.

52 D. E. Smiles, G. Wu and T. W. Hayton, *Inorg. Chem.*, 2014, **53**, 12683–12685.

53 C. Camp, O. Cooper, J. Andrez, J. Pecaut and M. Mazzanti, *Dalton Trans.*, 2015, **44**, 2650–2656.

54 P. L. Arnold, J. H. Farnaby, R. C. White, N. Kaltsoyannis, M. G. Gardiner and J. B. Love, *Chem. Sci.*, 2014, **5**, 756–765.

55 E. Askarizadeh, A. M. J. Devoille, D. M. Boghaei, A. M. Z. Slawin and J. B. Love, *Inorg. Chem.*, 2009, **48**, 7491–7500.

56 G. Givaja, A. J. Blake, C. Wilson, M. Schröder and J. B. Love, *Chem. Commun.*, 2003, 2508–2509.

57 T. Cantat, B. L. Scott and J. L. Kiplinger, *Chem. Commun.*, 2010, **46**, 919–921.

58 P. L. Arnold, C. J. Stevens, J. H. Farnaby, M. G. Gardiner, G. S. Nichol and J. B. Love, *J. Am. Chem. Soc.*, 2014, **136**, 10218–10221.

59 C. D. Carmichael, N. A. Jones and P. L. Arnold, *Inorg. Chem.*, 2008, **47**, 8577–8579.

60 I. Castro-Rodriguez, H. Nakai, P. Gantzel, L. N. Zakharov, A. L. Rheingold and K. K. Meyer, *J. Am. Chem. Soc.*, 2003, **125**, 15734–15735.

61 S. M. Mansell, J. H. Farnaby, A. I. Germeroth and P. L. Arnold, *Organometallics*, 2013, **32**, 4214–4222.

62 T. Arliguie, L. Belkhiri, S.-E. Bouaoud, P. Thuéry, C. Villiers, A. Boucekkine and M. Ephritikhine, *Inorg. Chem.*, 2009, **48**, 221–230.

63 M. Mancini, P. Bougeard, R. C. Burns, M. Mlekuz, B. G. Sayer, J. I. A. Thompson and M. J. McGlinchey, *Inorg. Chem.*, 1984, **23**, 1072–1078.

64 P. J. Fagan, J. M. Manriquez, E. A. aatta, A. M. Seyam and T. J. Marks, *J. Am. Chem. Soc.*, 1981, **103**, 6650–6667.

65 W. J. Evans, K. A. Miller, S. A. Kozimor, J. W. Ziller, A. G. DiPasquale and A. L. Rheingold, *Organometallics*, 2007, **26**, 3568–3576.

66 J. G. Brennan, R. A. Andersen and A. Zalkin, *Inorg. Chem.*, 1986, **25**, 1761–1765.

67 O. P. Lam, L. Castro, B. Kosog, F. W. Heinemann, L. Maron and K. Meyer, *Inorg. Chem.*, 2012, **51**, 781–783.

68 H. Binder, H. Loos, K. Dermentzis, H. Borrmann and A. Simon, *Chem. Ber.*, 1991, **124**, 427–432.

69 K. Wolfer, H. D. Hausen and H. Binder, *Z. Naturforsch., B: Anorg. Chem., Org. Chem.*, 1985, **40**, 235–239.

70 H. Binder, K. Diamantikos, H. D. Dermentzis and Z. Hausen, *Z. Naturforsch., B: Anorg. Chem., Org. Chem.*, 1982, **37**, 1548–1552.

71 W. Diamantikos, H. Heinzelmann, E. Rath and H. Binder, *Z. Anorg. Allg. Chem.*, 1984, **517**, 111–117.

72 A. J. Boutland, I. Pernik, A. Stasch and C. Jones, *Chem. Eur. J.*, 2015, **21**, 15749–15758.

73 A. F. R. Kilpatrick, J. C. Green and F. G. N. Cloke, *Organometallics*, 2015, **34**, 4816–4829.

74 J. Campora, E. Gutierrez, A. Monge, P. Palma, M. L. Poveda, C. Ruiz and E. Carmona, *Organometallics*, 1994, **13**, 1728–1745.